SPACE TELESCOPE SCIENCE INSTITUTE

INSTRUMENT SCIENCE REPORT

CAL/FOS-45

TITLE: FOS linearity corrections (revisited)

AUTHOR: D. Lindler and R. Bohlin DATE: August. 1988

ABSTRACT

Data taken during June and August 1984 and April 1988 show that the FOS diode non-linearity (paired pulse correction) can be modeled by:

$$x = \frac{y}{(1 - ty)} ,$$

Where y is the observed count rate (counts/sec) and x is the true count rate. The time coefficient t is constant (9.62 microsec) up to 52,000 observed counts per sec, which corresponds to a true input rate of about 100,000. Above 52,000 counts, t is modeled by:

$$t = q_o + q_1 (y - F)$$

where:

$q_o = 9.62 \times 10^{-6}$
$q_1 = 1.826 \times 10^{-10}$
$F = 52,000$

No significant diode to diode variation in the nonlinearity is seen below 100,000 true (input) counts/sec. Above this count rate the observed count rate varies from diode to diode by as much as ± 10%.

The accuracy of this model in predicting true corrected count rates should be better than 1% below 20,000 and degrading to about 5% for an average of many diodes at 100,000 true counts/sec.

The variation in the time constant above 52,000 observed counts may be caused by photocathode "fatigue". This variation is consistent with both the 1984 and 1988 red tube data The blue tube lacks data above 52,000 observed counts/sec.

If the variation in the time constant above 52,000 observed counts/sec is due to photocathode fatigue, our model may not be applicable to point source stellar data where the apertures are not fully illuminated.

DISTRIBUTION:

ISB
CSC
SDAS
SOGS
IDT

I. Introduction

The FOS detectors are two Digicons with 512 independent diodes and pulse counting channels. The counting circuitry of the detectors is not able to count all photoelectrons received. After recording a pulse from one event (electron) there is a recovery time before a second event can be detected. Photon arrivals are described by Poisson statistics. As the mean time interval between events decreases, a significant number of events will be separated by less than the recovery time. These "paired pulses" would be counted as a single event, causing the observed counting rate to be less than the actual rate of photoelectron events. As the mean interval becomes shorter than the recovery time, the detector would never recover and no count would be recorded. To avoid this paralysis at very high counting rates, a "dead time" is built into the counting circuitry, which is chosen to be longer than the recovery time. After counting an event, the channel is turned off for one dead time interval.

An analytical model of the observed count rate as a function of the actual count rate may be derived as follows: let y be the observed count rate and t the dead time. For a time interval T the number of events counted will be Ty. The total time the circuit is "dead" is tTy. The total time the circuit is "alive" and can count events is T - tTy. If x is the actual rate of events the total number of events counted is given by (T - tTy) x. (The time the circuitry is enabled times the mean rate of events).

Therefore:

$$Ty = (T - tTy)x \qquad (1)$$

or equivalently:

$$x = \frac{y}{1 - ty} \qquad (2)$$

The FOS dead time is 10 clock pulses of 0.977 microsec from a 1.024 megahertz clock. Depending on when an event arrives, the dead time can vary from 9 x 0.977 or 8.79 microsec (if the event occurs immediately before a clock pulse) to 10 x 0.977 or 9.77 microsec (if the event occurs immediately after a clock pulse).

II. Data

The non-linearities in the counting rates were measured by holding the light output from the optical simulator constant while changing the light input to the FOS detectors by known amounts . The light input to the detectors was varied by selection of different entrance apertures.

Data were taken in June and August 1984 and April 1988 using the ambient ST optical simulator with a tungsten lamp. An analysis of the earlier data is in Lindler and Bohlin (1986). Grating H57 on the red tube and grating H40 on the blue tube were used. For

each detector data were taken for all entrance apertures. For the blue tube, observed counting rates varied from less than 100 counts/sec (aperture A4, 0".1 square) to approximately 50,000 (aperture A1, 4".3 square). Count rates for the red tube varied from less than 1000 counts/sec (A4) to 70,000 counts/sec (A1). Observations were repeated for all apertures with a 10% neutral density filter inserted to decrease the input count rate by approximately a factor of 10, in order to compute the relative aperture sizes. Because of the decreased count rates, the neutral density filter minimized the effect of the nonlinearity on the aperture size computations.

All data were taken with no overscanning to allow analysis of diode to diode variations. To avoid filter/grating wheel repeatability problems, all data for each detector were taken without moving the grating wheel. Y-bases were checked and adjusted immediately prior to taking the data to minimize the effects of spectral motion due to thermal changes and high voltage settling. This Y-base check was omitted for the 1984 red tube data.

III.Data Reduction

The first step in the data analysis was to determine the relative aperture sizes versus diode number (or equivalently, wavelength). Data taken with the 10% neutral density filter were corrected for non-linearities using a preliminary paired-pulse model with a time coefficient of 9.43 microsec. Since count rates were small (<10,000 counts/sec), errors resulting from inaccuracies in the model were not significant. Aperture sizes relative to the B2 (0.3 arcsec circle) were computed for each diode by dividing the corrected count rate of all apertures by the corrected count rate of the B2 aperture. Because of significant diffraction losses for the smaller apertures that cause the ratios to vary as a function of wavelength, a linear fit to each ratio versus diode number was used as the relative aperture size.

The second step was to compute the true count rate for each aperture when the neutral density filter was not in place. The small B2 aperture with a counting rate of 7,500 counts/sec for the red tube and 650 for the blue tube was used as a reference. The data for the B2 aperture were corrected with the preliminary paired pulse model. The expected count rates for the other apertures were computed for each diode by multiplying the corrected B2 spectrum by the relative aperture sizes. Using data from all apertures, a table of true counts, X, versus observed counts, Y, was created. For each data point, a dead time was computed by:

$$t = \frac{1}{y} - \frac{1}{x} \quad , \qquad (3)$$

which is equation (2) solved for t.

The final step is to compute coeficients q_o, q_1, and F for the paired pulse model:

$$x = \frac{y}{(1-ty)} \qquad (4)$$

$$t = \begin{cases} q_o \text{ for } y \leq F \\ q_1 + (y - F) \text{ for } y > F \end{cases}$$

where

x is the expected count rate
y is the observed count rate
q_o is the time constant for observed counts less than F
q_1 is the slope of the linear model for the time constant for observed counts greater than F.
F is the observed count threshold, where the time coefficient is no longer a constant value.

F is chosen as 52,000 by visual examination of the plot of t versus y (see Figure 1). The value of q_o is the average of t for data points with 25,000 $\leq$y <52,000. The data points below 25,000 have a significant scatter resulting from counting statistic errors and photocathode granularity.

The value of q_1 is the slope of the least squares linear fit of the data points with y > 52,000. The fitted line is constrained to pass through the point y = 52,000 and t = q_o. The entire process is repeated using the new q_o and q_1 values to correct the low count rate data in the relative aperture size computation until q_o and q_1 converge.

IV. Analysis

Coefficients for the model are computed for both the 1984 and 1988 data.

	1984		1988	
q_o	9.43×10^{-6}	sec	9.62×10^{-6}	sec
q_1	2.568×10^{-10}	sec/count	1.826×10^{-10}	sec/count
F	51,000	counts	52,000	counts

The points of the time coefficients computed using equation 3 are shown in Figures 1 to 4. The model for the time coefficients is shown as a solid line. Only the central 300 diodes were used for the August 1984 red tube, since the absence of a y-base check caused significant repeatability problems at the ends of the diode array.

The other data with verified y-bases showed much better repeatability of count rates.

When q_o is computed separately for each tube, no significant variation is seen: The April 1988 data has a $q_o = 9.62 \times 10^{-6}$ sec for the red tube and $q_o + 9.61 \times 10^{-6}$ sec for the blue tube. No comparison of q_1 could be performed, since the blue count rates never exceeded 50,000 observed counts/sec.

Figures 5 to 8 show plots of the observed count rates versus the true count rates. Overplotted as a solid line is the non-linearity model.

The increased time constant above 50,000 counts may be due to photocathode fatigue. Figures 9 and 10 shows plots of the spectra from all apertures versus diode number. The central part of the aperture C3 (2 x 2 arcsec with occulting bar) shows a flattening of the spectrum in 1984 with a slight dip in the center, which suggests that the fatigue in the center of the photocathode is greater than at the sides. The spectrum for the A1 aperture begins to show the correct curvature indicating that fatigue also becomes prominent at the edges at higher count rates. If the fatigue effect is due to the limited current carry capacity of the photocathode substrate, then the results presented here may overestimate the importance of fatigue in the flight situation. The 2.0 and 4.3 arcsec apertures are taller than the 1.4 arcsec height of the diodes. Therefore, more current is drawn in the laboratory calibration with fully illuminated apertures than is drawn for the same count rate from a stellar point source. Since the evidence for fatigue is less convincing in 1988, another explanation may be correct.

The large scatter of the data for aperture C3 for rates around 60,000 counts per second in Figures 9 and 10 indicates that the non-linearity at higher count rates is diode dependent. This diode dependent behavior may be due to a pulse "pile up" at high count rates. Both noise pulses and pulses from photon events have a width and shape associated with them that may vary from channel to channel. At these high count rates, changes to the discriminator levels will effect the linearity. As the true count rate increases above 300,000 counts/sec, the amount of scatter in observed count rates decreases due to increased saturation. All channels should saturate fully at the inverse of the dead time, which is an observed rate of about 100,000 counts/sec. In fact, the maximum observed rate is about 80,000. Despite the good repeatability of diode-to-diode variation at high count rates as shown in Figure 11, there are no plans to implement a diode dependent linearity correction at this time. Figure 11 shows the same set of values taken 4 years apart. Despite the replacement of the red tube during this period, the data show approximately the same pattern. Thus, the scatter is not a result of photocathode or diode effects but is in the counting electronics, which were not changed.

V. Error Analysis

Figures 12-15 show plots of the error in the model versus true count rates. The scatter below 80,000 counts per second can be attributed to counting statistics and photocathode granularity. Systematic variations at count rates under 80,000 counts/second can be attributed to either inadequacies in the model or to spectral motions, which causes loss of light when the spectra are not centered on the diode array. Repeatability checks using the C1 aperture showed variations due to spectral motions on the order of 1% for the 1984 data and 0.2 % for the 1988 data. Since Figures 12-15 provide only upper limits to the errors below 80,000 counts per second, an alternate approach is to estimate an error in the time constant. A conservative estimate is 0.5 microsec.

An error of 0.5 microsecond leads to the following errors in the computation of true counts from observed counts.

true count rate	observed count rate	error
100	100	.005%
1,000	900	.05 %
5,000	4,800	.25 %
10,000	9,100	.5 %
20,000	17,000	1.0 %
30,000	23,000	1.5 %
40,000	29,000	2.0 %
80,000	46,000	4.0 %

The data for the red detector is consistent with the blue detector up to 80,000 counts/sec. Above 80,000, the red-side errors can be estimated from Figures 12 and 13.

Red Side Only

true count rate	observed count rate	error
100,000	51,000	5%
150,000	57,000	25%
200,000	60,000	50%

If the increase in the time constant above 100,000 true counts/sec is due to photocathode fatigue, results for the red tube may not be applicable to the observation of point sources in orbit.

The algorithm with the constants q_0, q_1, and F listed in the abstract will be used to reduce the initial flight data from the FOS.

REFERENCE

Lindler, D., and Bohlin,R. 1986, CAL/FOS-25, STScI.

FIGURE CAPTIONS

Fig. 1 to 4 Computed time constant versus observed count rate. The model for the time constant is overplotted as a solid line. The scatter in the 1988 data is larger than in the 1984 data, since shorter integration times were used in 1988, when no attempt was made to find different linearity corrections for different diodes.

Fig. 5 - 8 Comparison between the data and the computed non-linearity model.

Fig. 9 - 10 Observed count rate for the Red tube and grating H57 for all apertures with no filter.

Fig. 11 Repeatability of the diode to diode variations for the red tube, aperture C3.

Fig. 12 - 15 Percent error of the true count rate, as derived from the difference between the model and the computed true count rate for each data point.

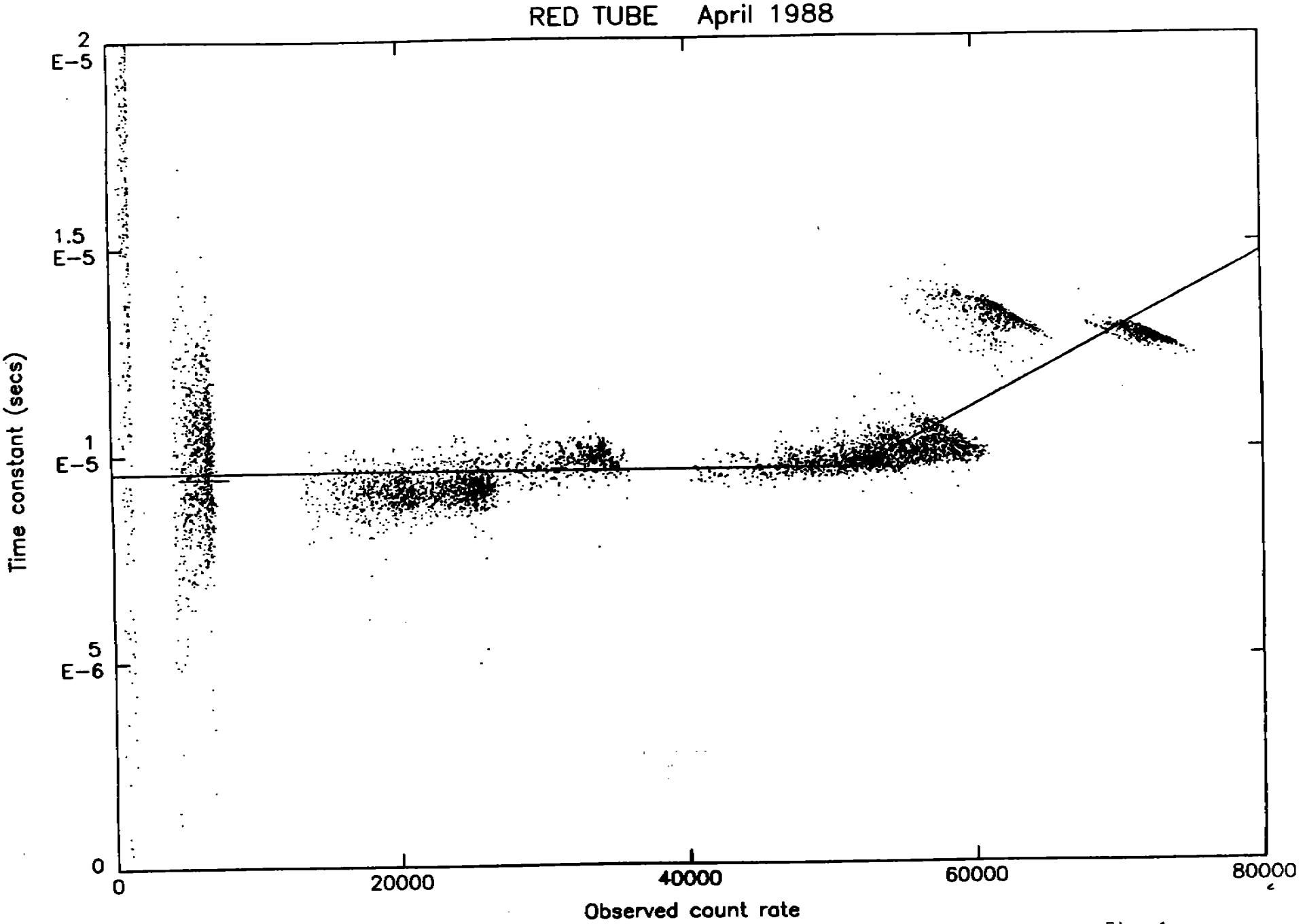
RED TUBE April 1988
2 E-5
1.5 E-5
1 E-5
5 E-6
0
Time constant (secs)
0
20000
40000
60000
80000
Observed count rate

Fig. 1

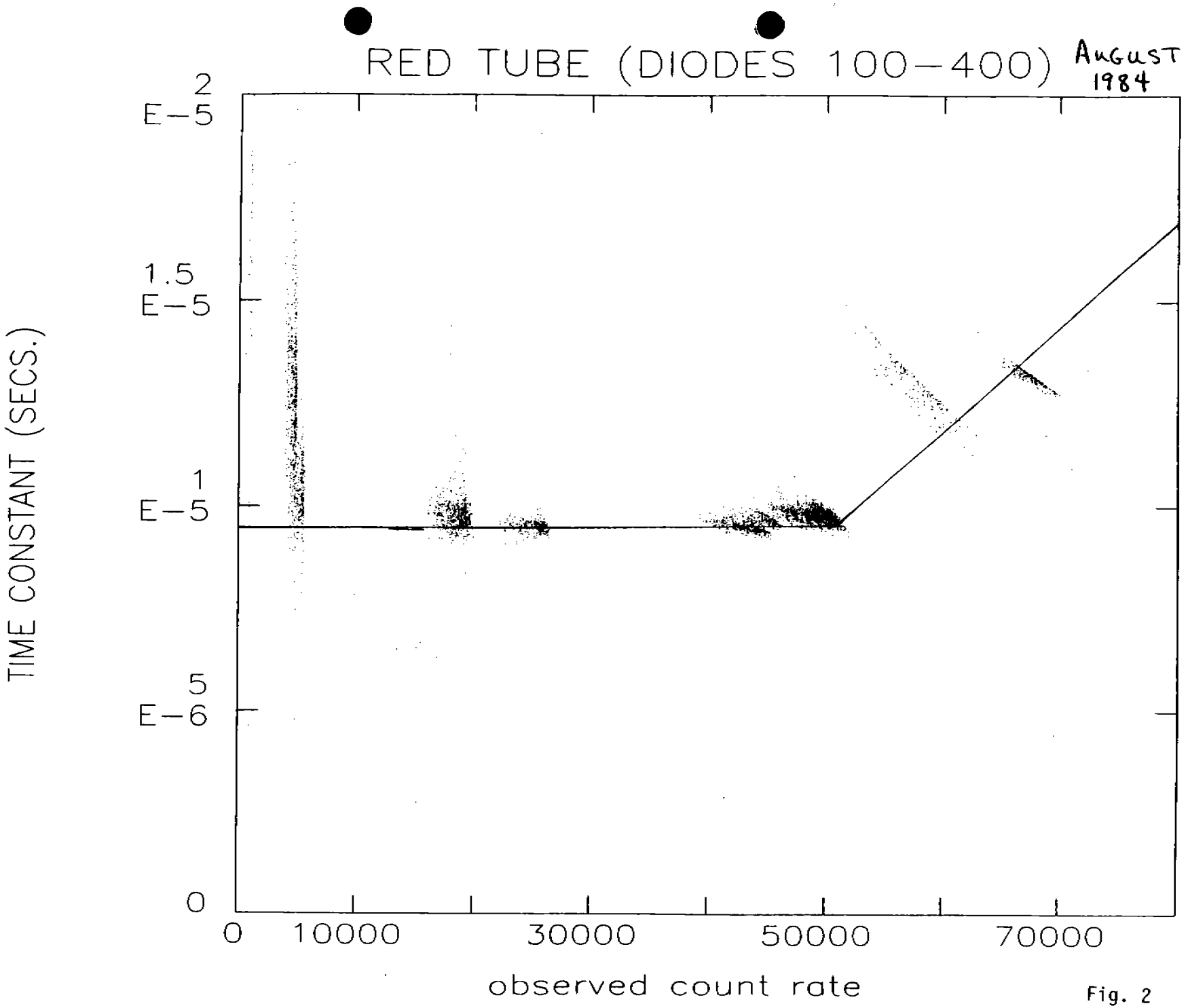
RED TUBE (DIODES 100–400)
AUGUST 1984
TIME CONSTANT (SECS.)
2 E–5
1.5 E–5
1 E–5
5 E–6
0
0
10000
30000
50000
70000
observed count rate

Fig. 2

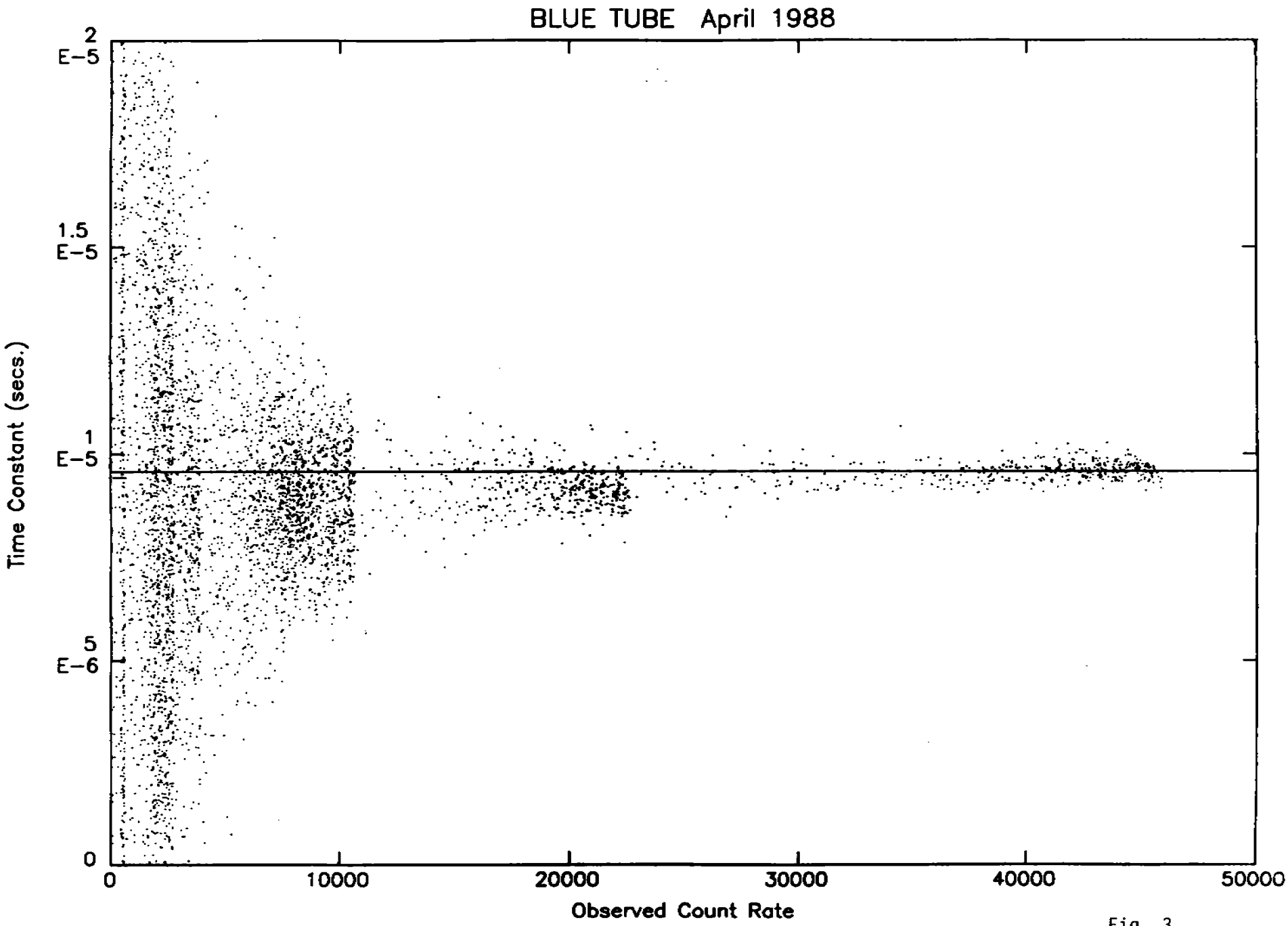
BLUE TUBE April 1988
2 E-5
1.5 E-5
1 E-5
5 E-6
0
Time Constant (secs.)
0
10000
20000
30000
40000
50000
Observed Count Rate

Fig. 3

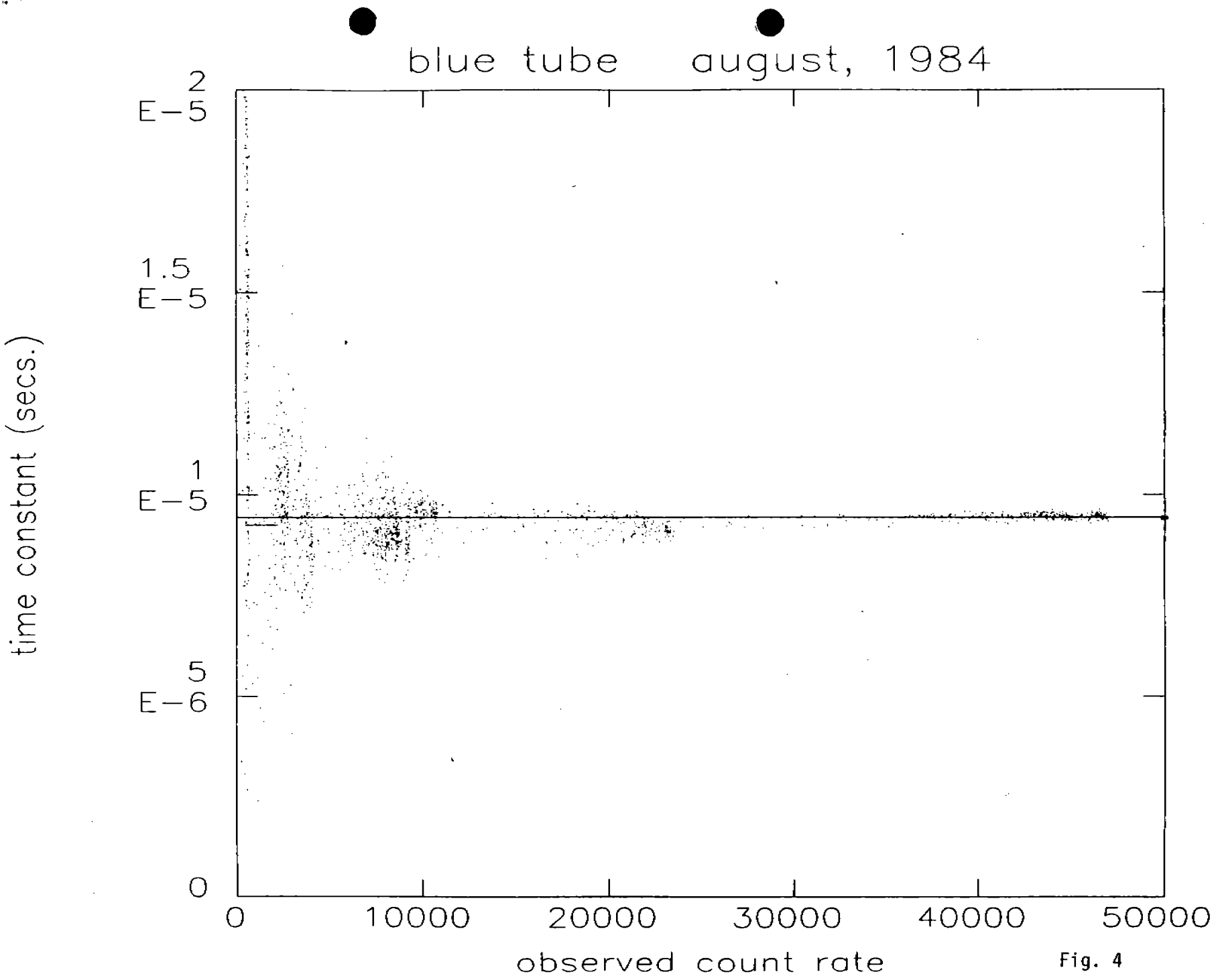
blue tube august, 1984
2 E-5
1.5 E-5
1 E-5
5 E-6
0
time constant (secs.)
0
10000
20000
30000
40000
50000
observed count rate

Fig. 4

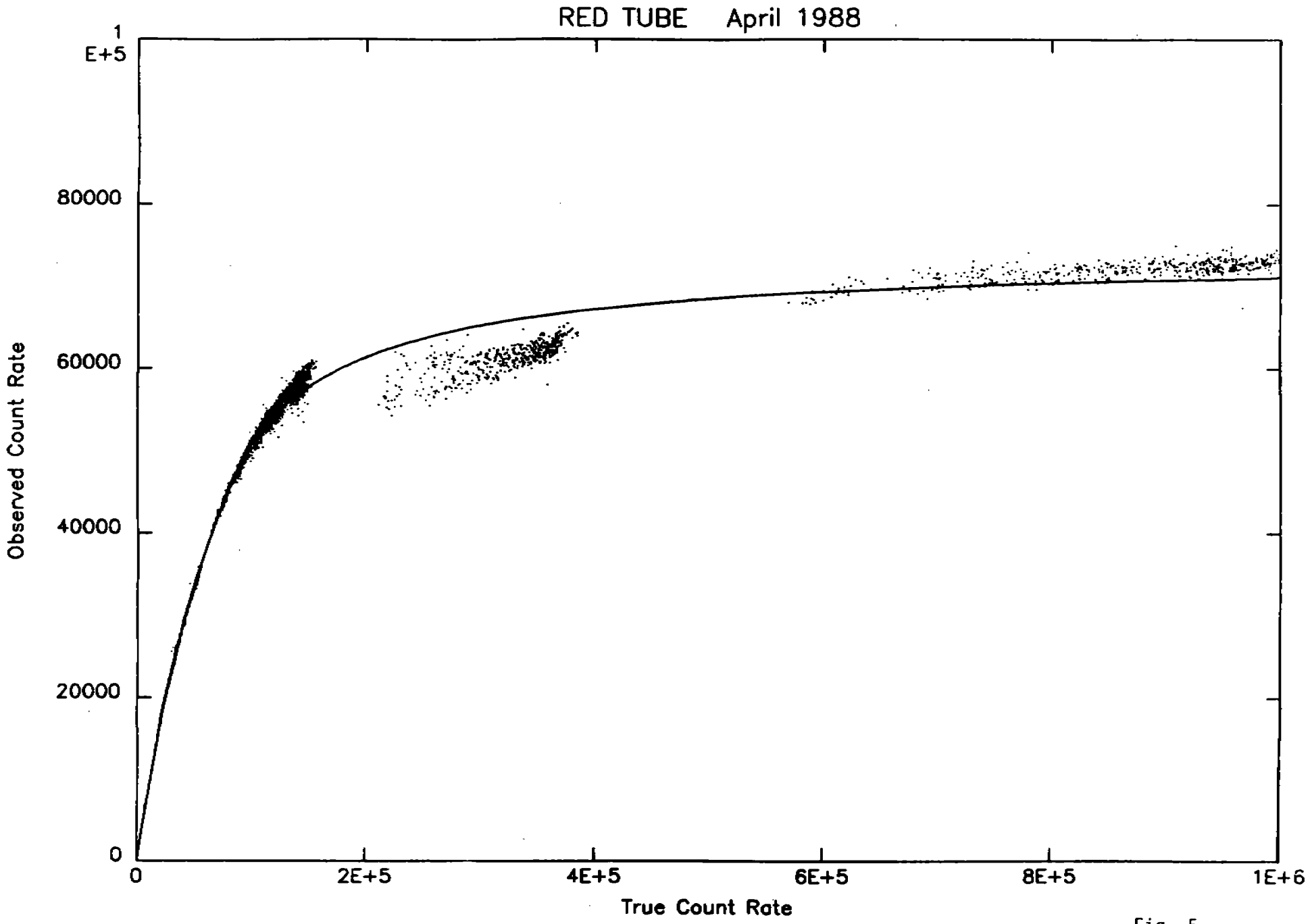
RED TUBE April 1988
1 E+5
80000
60000
40000
20000
0
Observed Count Rate
0
2E+5
4E+5
6E+5
8E+5
1E+6
True Count Rate

Fig. 5

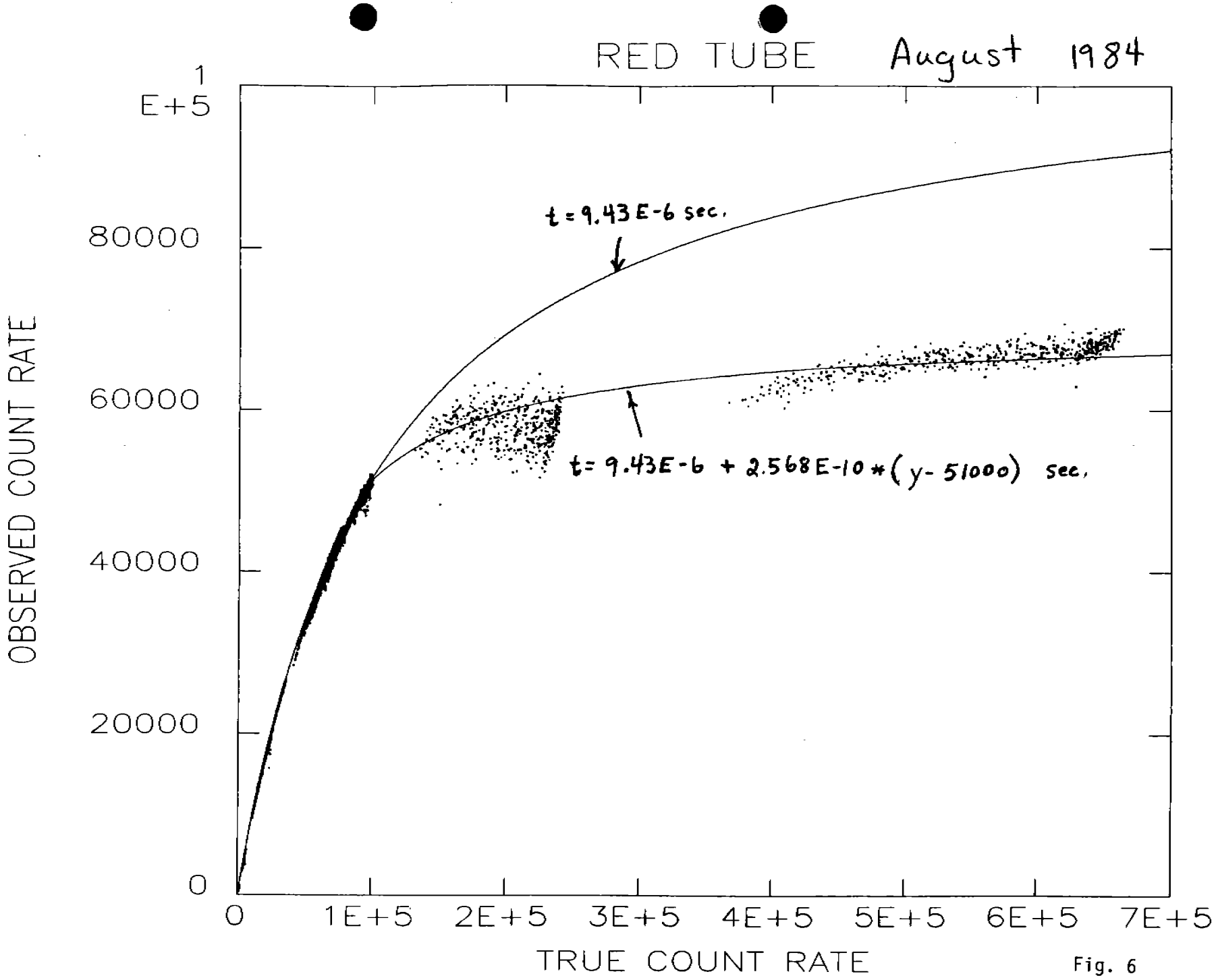
RED TUBE August 1984
1 E+5
80000
60000
40000
20000
0
OBSERVED COUNT RATE
t = 9.43 E-6 sec.
t= 9.43E-6 + 2.568E-10 * (y- 51000) sec.
0
1E+5
2E+5
3E+5
4E+5
5E+5
6E+5
7E+5
TRUE COUNT RATE

Fig. 6

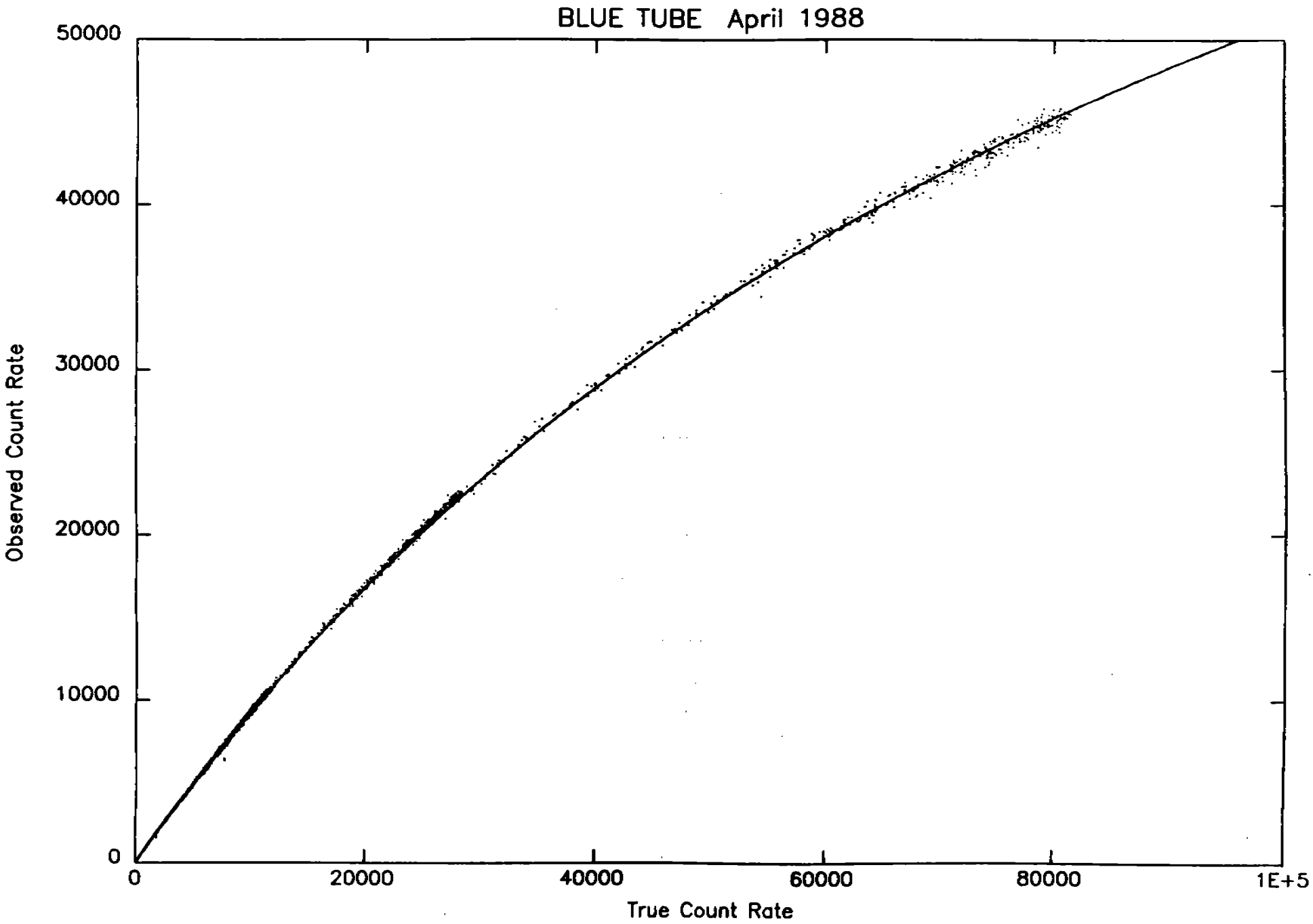
BLUE TUBE April 1988
50000
40000
30000
20000
10000
0
Observed Count Rate
0
20000
40000
60000
80000
1E+5
True Count Rate

Fig. 7

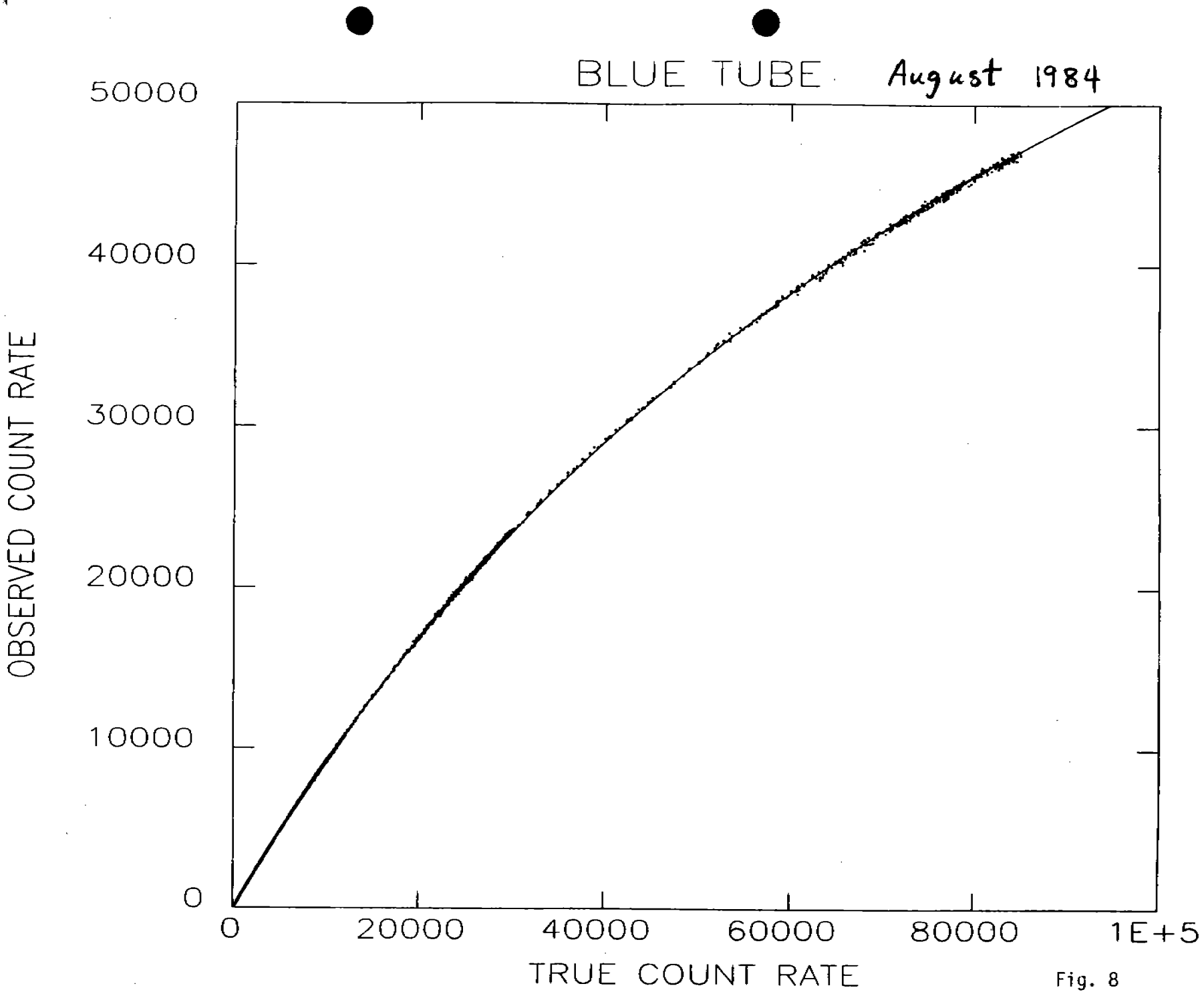
BLUE TUBE August 1984
50000
40000
30000
20000
10000
0
OBSERVED COUNT RATE
0
20000
40000
60000
80000
1E+5
TRUE COUNT RATE

Fig. 8

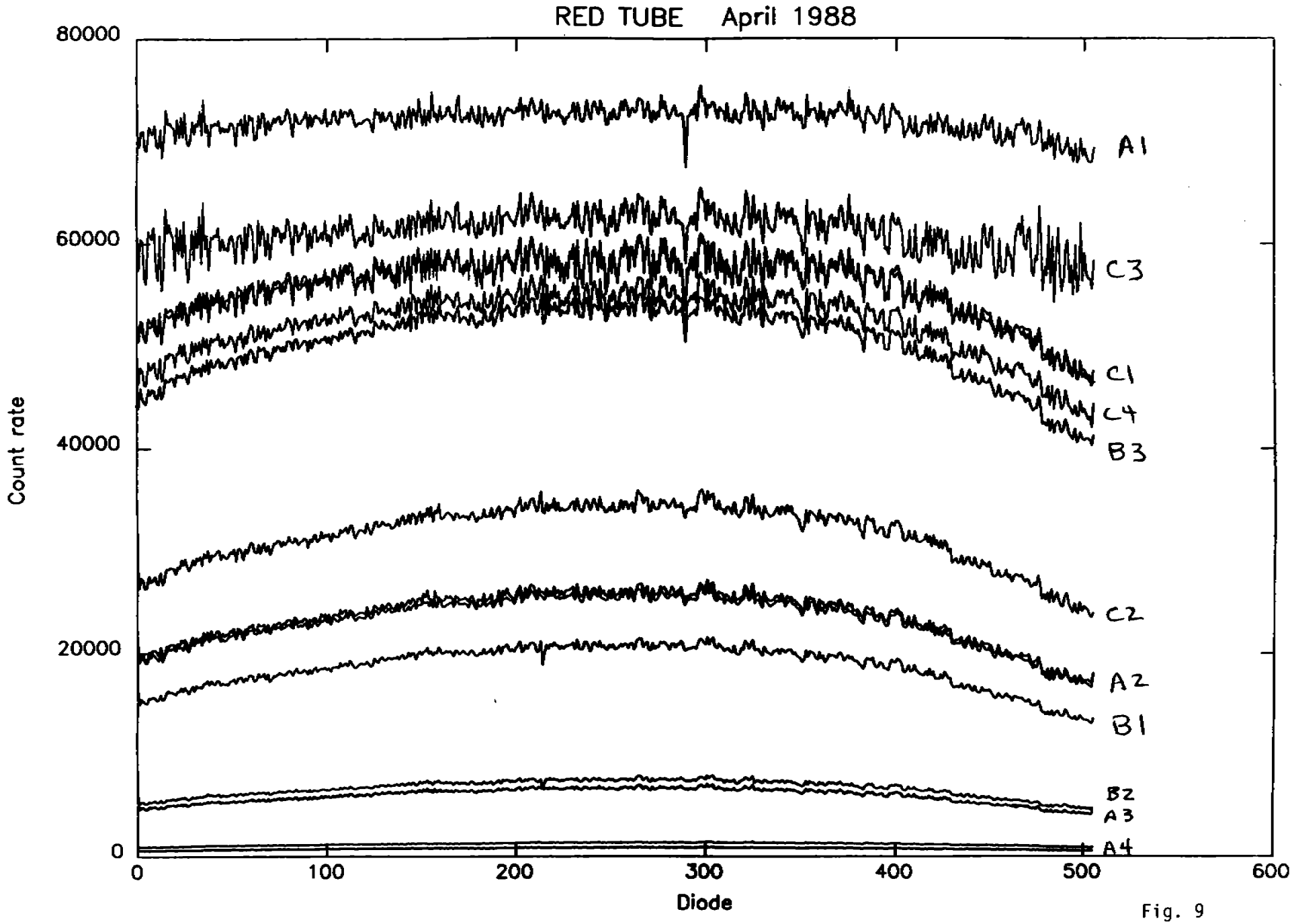
RED TUBE April 1988
80000
60000
40000
20000
0
Count rate
0
100
200
300
400
500
600
Diode
A1
C3
C1
C4
B3
C2
A2
B1
B2
A3
A4

Fig. 9

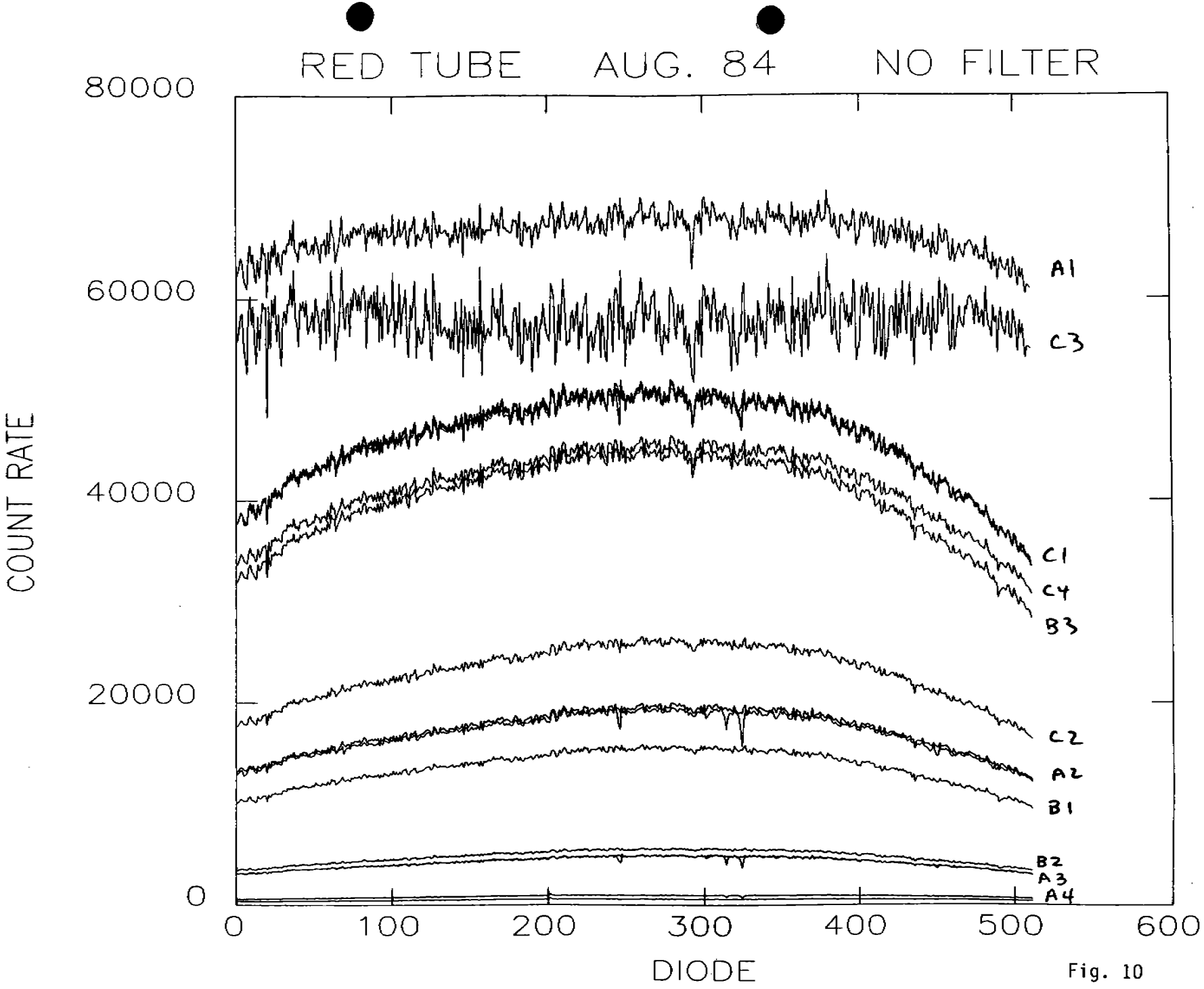
RED TUBE AUG. 84 NO FILTER
80000
60000
40000
20000
0
COUNT RATE
A1
C3
C1
C4
B3
C2
A2
B1
B2
A3
A4
0
100
200
300
400
500
600
DIODE

Fig. 10

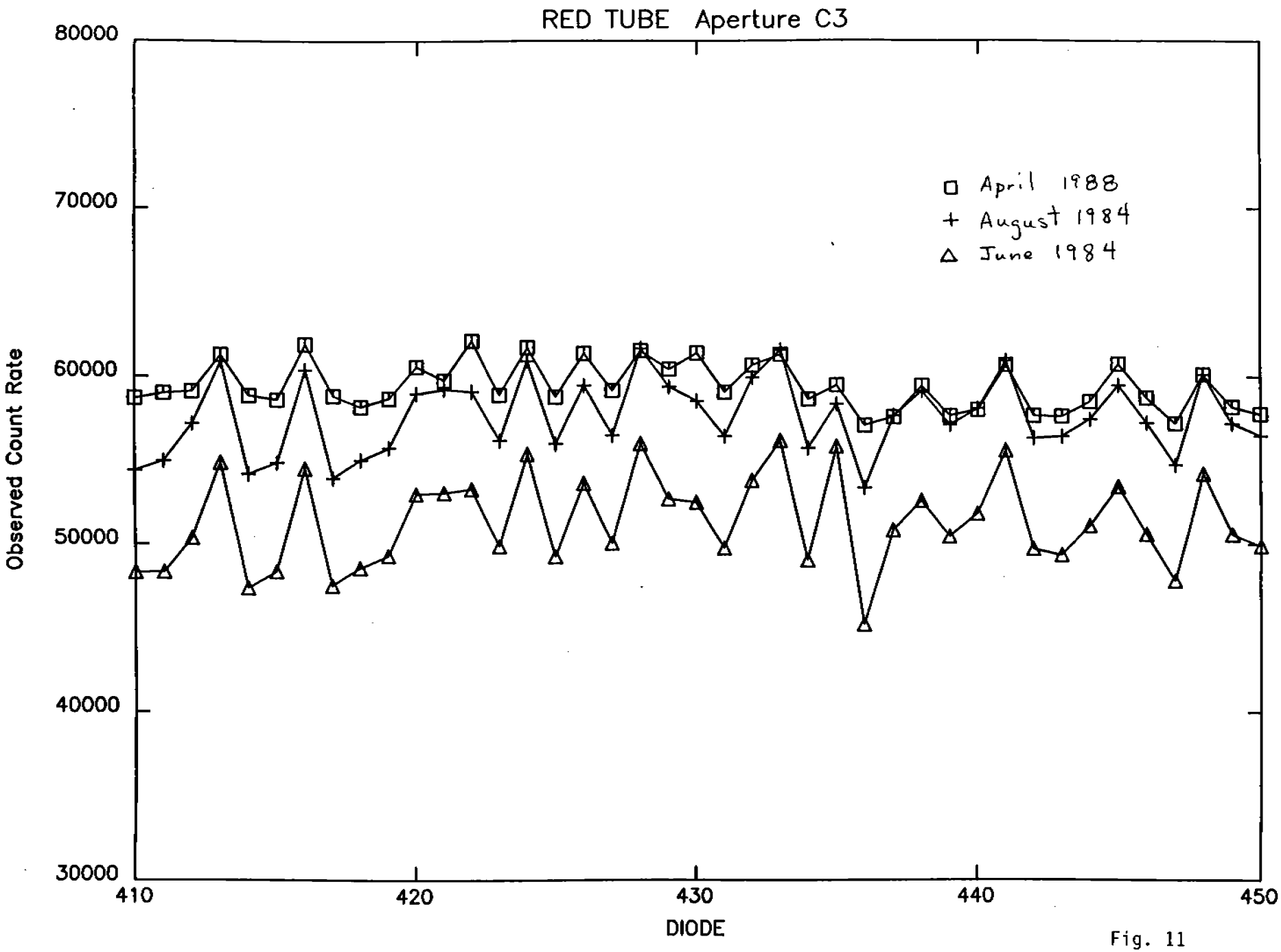
RED TUBE Aperture C3
80000
70000
60000
50000
40000
30000
Observed Count Rate
410
420
430
440
450
DIODE
April 1988
August 1984
June 1984

Fig. 11

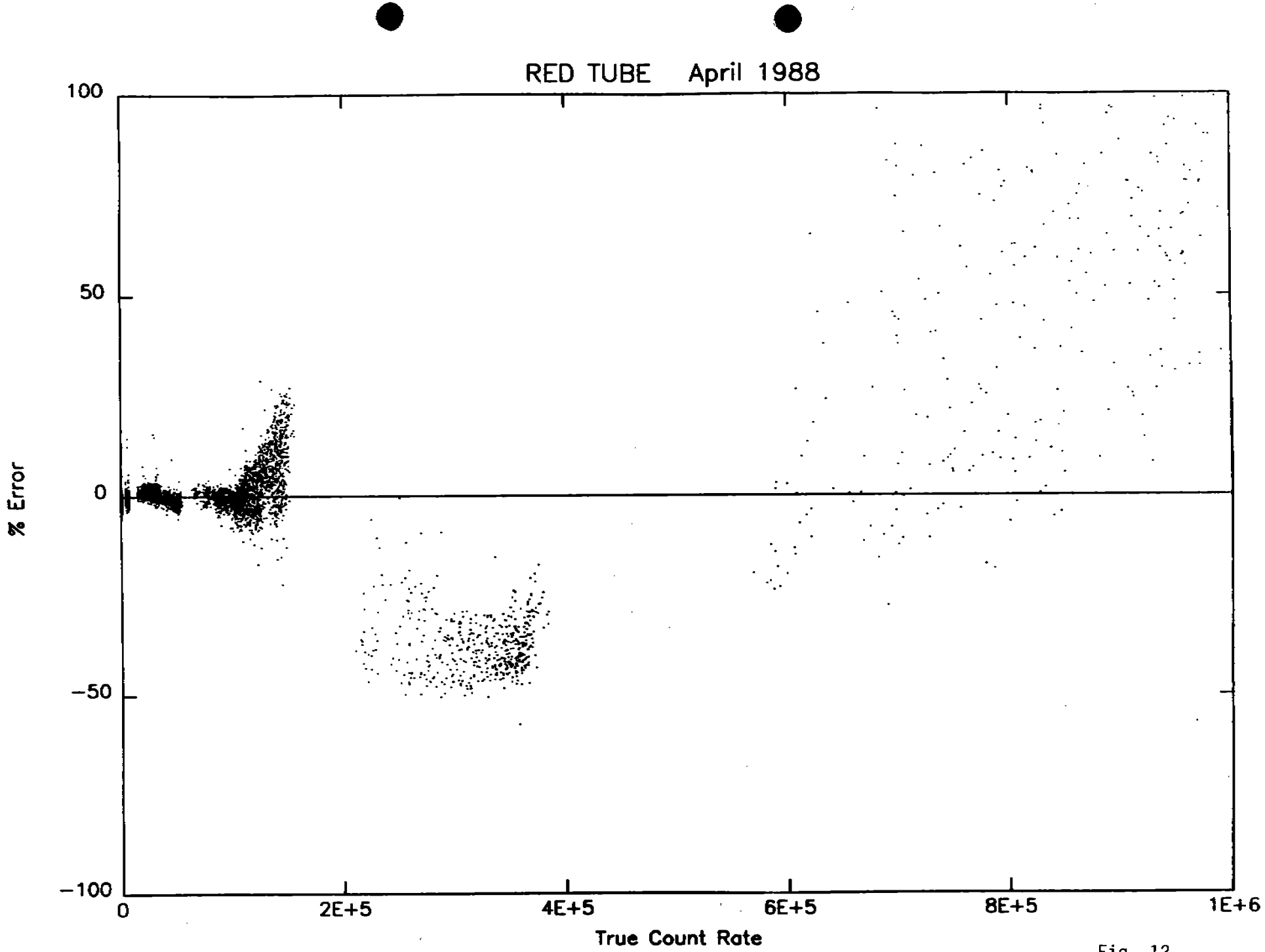
RED TUBE April 1988
100
50
0
−50
−100
% Error
0
2E+5
4E+5
6E+5
8E+5
1E+6
True Count Rate

Fig. 12

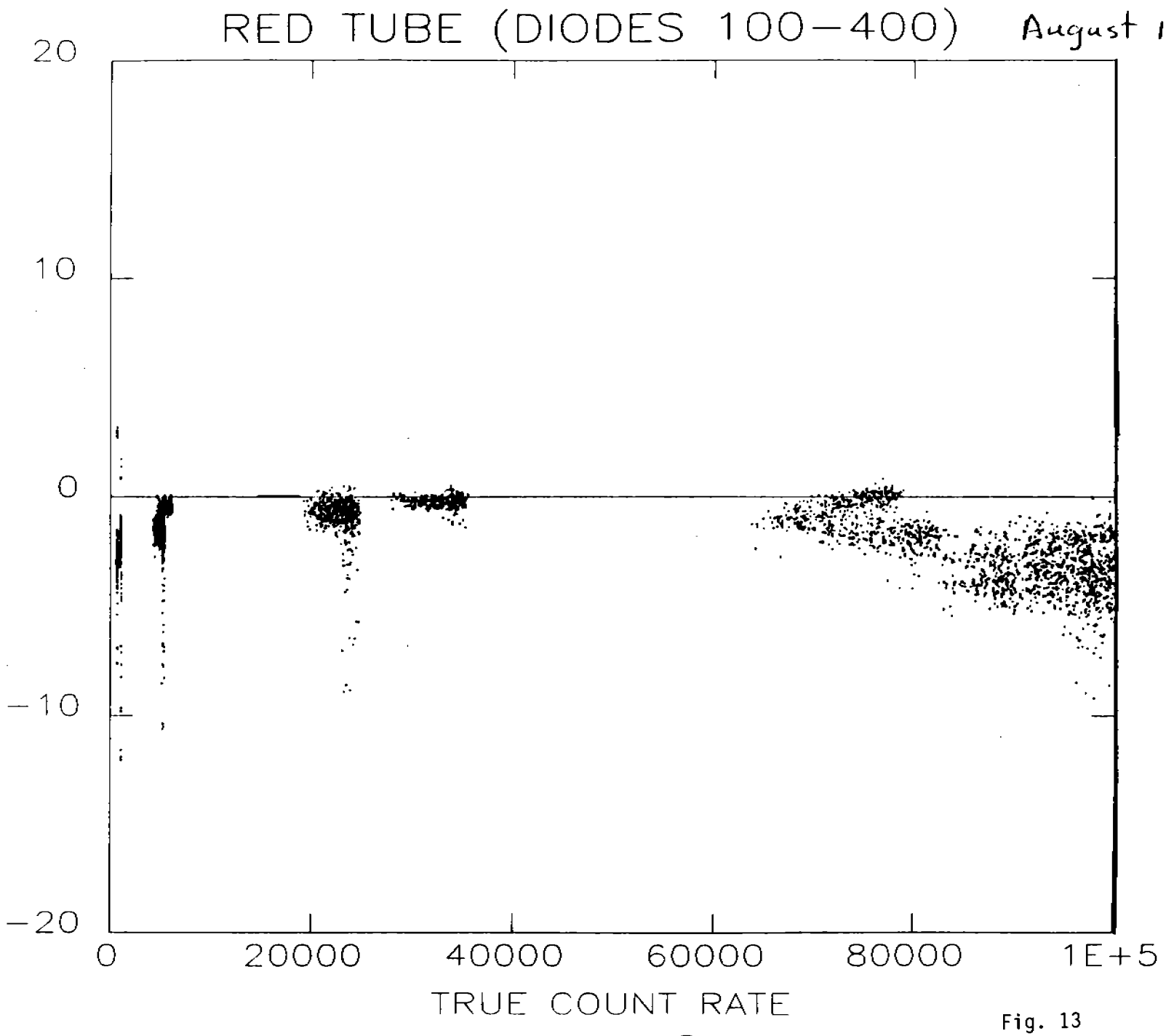
RED TUBE (DIODES 100–400) August 1984
20
10
0
–10
–20
% ERROR
0
20000
40000
60000
80000
1E+5
TRUE COUNT RATE

Fig. 13

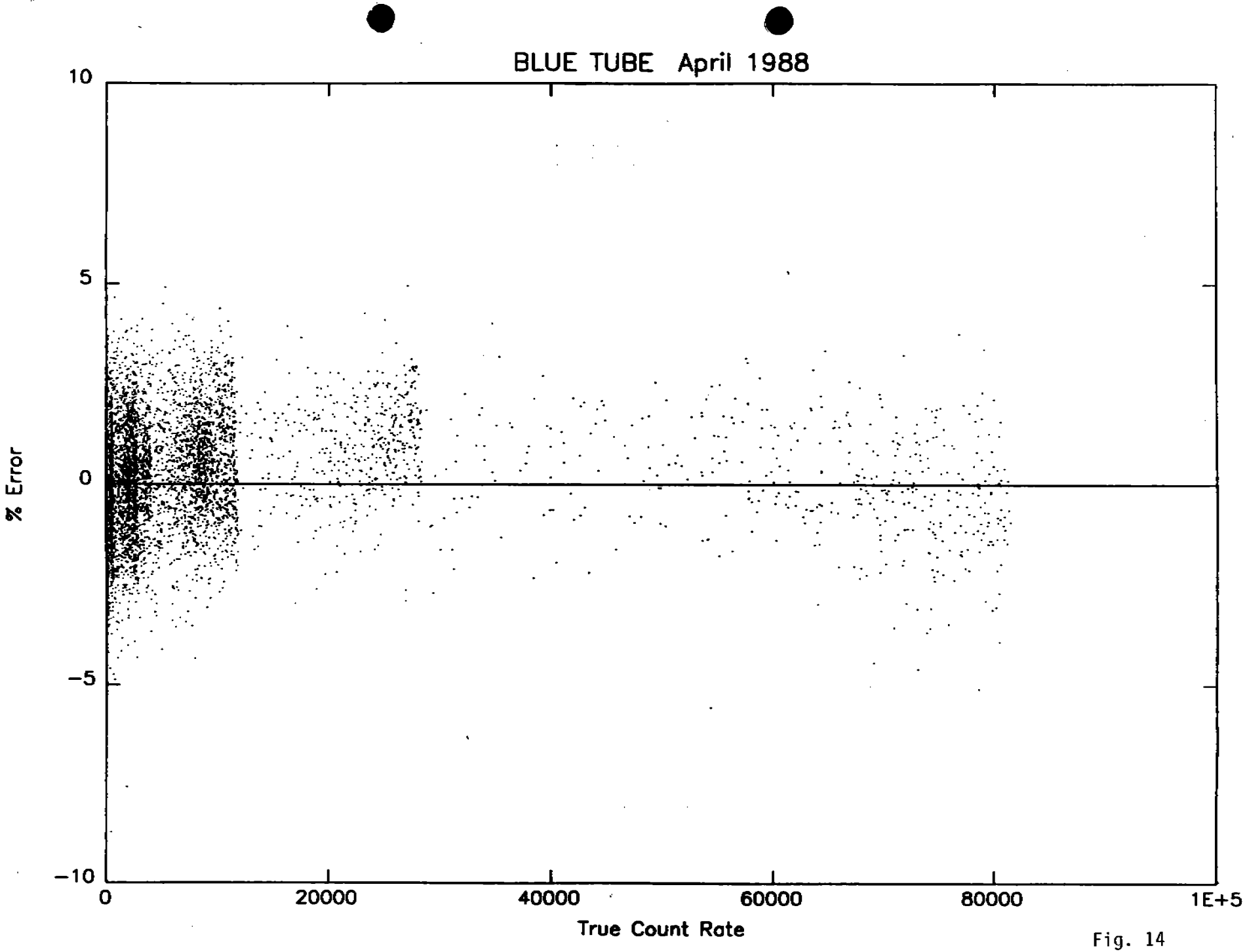
BLUE TUBE April 1988
10
5
0
−5
−10
% Error
0
20000
40000
60000
80000
1E+5
True Count Rate

Fig. 14

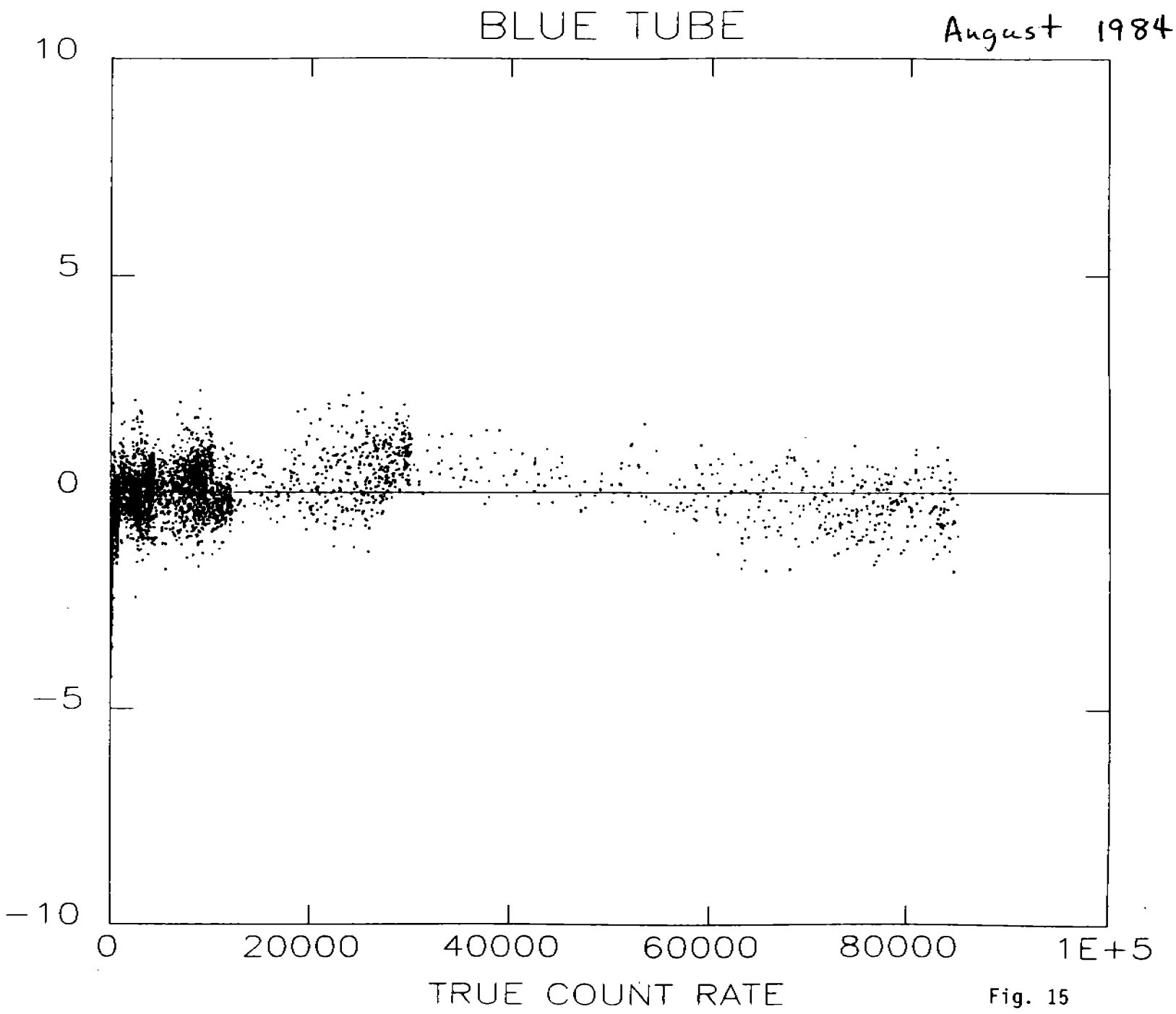
BLUE TUBE
August 1984
10
5
0
−5
−10
% ERROR
0
20000
40000
60000
80000
1E+5
TRUE COUNT RATE

Fig. 15